Design and Optimization of a High Temperature Microheater for Inkjet Deposition

Austin VanHorn, Wenchao Zhou
The AM³ Lab, Department of Mechanical Engineering, University of Arkansas at Fayetteville
Fayetteville, AR, United States of America; email: zhouw@uark.edu

REVIEWED

ABSTRACT

Inkjet deposition has become a promising additive manufacturing technique due to its fast printing speed, scalability, wide choice of materials, and compatibility for multi-material printing. Among many different inkjet techniques, thermal inkjet, led by Hewlett-Packard and Canon, is the most successful inkjet technique that uses a microheater to produce a pressure pulse for ejecting droplets by vaporizing the ink materials in a timespan of microseconds. Thermal inkjet has been widely adopted in many commercial 3D inkjet printers (e.g., 3D Systems ProJet X60 series) due to its low cost, high resolution, and easy operation. However, the viscosity of the printable materials has been limited to less than 40cP due to insufficient energy provided inside the nozzle to overcome the viscous dissipation of energy. This paper presents a study on the design and optimization of a high temperature microheater with a target heating temperature of more than 600˚C (compared to ~300 ˚C for current printhead) to increase the energy supply to the nozzle. The benefits are fourfold: 1) higher temperature will lead to faster vaporization of ink and thus higher jetting frequency and print speed; 2) higher temperature will make it possible for jetting materials with higher boiling points; 3) higher temperature will reduce the viscosity of the ink and thus the viscous dissipation of energy; 4) higher energy supply will increase the magnitude of the pressure pulse for printing more viscous materials. In this paper, a high temperature microheater was designed with the following objectives: to reduce thermal stress in heaters, and to minimize uneven heat distribution. A literature survey was first conducted on design, fabrication, and operation of thin-film resistive microheaters. A multiphysics numerical model was then developed to simulate electrical, thermal, and mechanical responses of the microheater. The model was validated by comparison to experimental data and existing models obtained from literature. With proper parameterization of the design geometry, the geometry of the microheater is optimized using a particle swarm optimization method. Results show the optimized high temperature microheater successfully operates at temperatures in excess of 600˚C. The design optimization enabled better characteristics for even heat distribution and minimizing stress. The design approach can serve as a fundamental means of design optimization for microheaters.

I. INTRODUCTION

Thermal inkjet has become a promising additive manufacturing technology due to its printing speed, low cost to fabricate, and fine printing resolution. It uses a microheater to produce a pressure pulse for ejecting droplets by vaporizing the ink materials in a timespan of microseconds. The microheater in the current thermal inkjet printhead typically operates at ~300°C [1] and the viscosity of printable materials is limited up to ~40cP [2]. Increasing the operating temperature of the microheater may offer multiple benefits, including higher jetting frequency and wider choice of materials with high viscosity and boiling points. Extensive research has been conducted on microheater development, such as fabrication, material properties, temperature limits, failure modes, and sustainability [3-11]. Progress has also been made on development of high temperature microheaters that can reach above 600 ˚C. Simulation has been used to predict the behaviors and optimization has been performed through iterative

simulations and experiments [11, 12]. However, little research has been reported on systematic approach for optimization of microheater geometry. In this paper, a constrained particle swarm optimization method, in combination with finite element simulations, is developed for optimization of a high temperature microheater that can operate at 600 ˚C, with design objectives to minimize uneven temperature distribution and thermal stress under certain design constraints. This study first presents a literature review on the current status of microheater design. It then proceeds into the development of a numerical model for simulating microheater operation. The numerical model is validated with experimental data from literature [9, 10]. With proper parameterization of the microheater geometric design, the validated numerical model is used to evaluate the designs with respect to the design objectives and a particle swarm optimization method is developed to find the optimal microheater geometry in a constrained design space.

II. LITERATURE REVIEW

Many research efforts were reported on thin-film resistive heaters (microheaters). This section is to provide a review of the state of the art of microheater technology and identify the research gap.

A. History and Motivation

James Prescott Joule initiated the first research conducted in resistive heating in 1841 which was later followed Hienrich Lenz in 1842. This method of heating did not get accepted by the Royal Society in London until 1849 when Michael Farraday sponsored the findings, which soon after led to James Joule's acceptance in the Royal Society [13]. Since then resistive heaters have found their way into many designs. One such application of resistive heating is thermal inkjet deposition. HP first introduced thermal inkjet technology in 1984 with their dot-matrix printer which miniaturized inkjet technology with higher quality, lower power, and quieter operation [14]. Current microheaters in thermal inkjet printers typically operate at ~300°C [1], which limits the ability to print materials with higher viscosity and higher boiling points. Higher temperatures will increase the pressure pulse from thermal inkjet printers and create quicker vaporization of materials therefore higher frequency for droplet generation.

B. Microheater Design

A microheater is a sophisticated MEMS device and its operation involves multiple physics, (electrical, mechanical, and thermal) as well as materials and geometric designs. Classical design of a microheater consist of four elements [15]: 1.) conductive pad, 2.) resistive heating element, 3.) substrate, 4.) oxidation passivation layers. A typical configuration is shown in Figure 1.

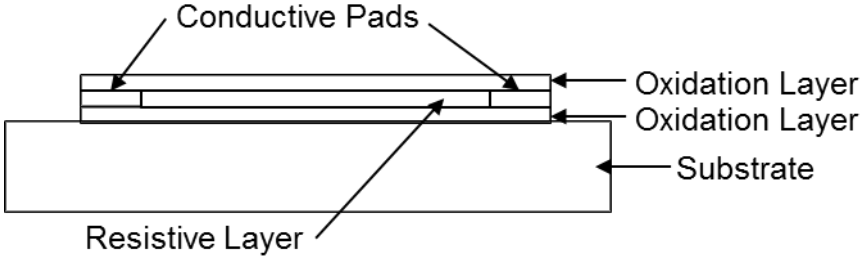

Figure 1-Schematic of the Four Basic Elements of a Microheater

The actual configuration of microheaters however, is ultimately based on the parameters and objectives trying to be reached with a particular design. One of the parameters established

for our design is to reach temperatures of 600°C. Much research has been done on microheaters capable of reaching temperatures of 600°C, which involves materials, fabrication, modeling, and design.

1) Materials

Many materials have been researched in literature for the four components used in a typical microheater configuration. The substrate provides the foundation for the microheater. Typical materials used are glass [10], silicon [8], ceramics [9], and stainless steel [16]. Silicon and ceramics typically can handle higher ranges of temperatures than steel and glass [16]. Ceramics like alumina typically have a high thermal conductivity creating high power consumption [9, 17]. However, Low Temperature Cofired Ceramics (LTCC) are a composite ceramic/glass material typically offering much lower thermal conductivity enabling power savings [9]. Stainless steel has higher thermal conductivity, but is often chosen because it is inert, robust, and has many well defined microfabrication techniques [16]. Silicon is a frequently chosen material used for substrates due to its ability to operate at 1000ºC temperatures for prolonged periods of time and high thermal conductivity enabling quick thermal response times [8].

The resistive layer is where the main source of resistive heating occurs. Resistive materials that can operate at temperatures above 600°C are needed for high temperature microheaters. Some of the studied materials include Platinum (Pt) [9, 18, 19], Titanium (Ti) [10, 15], SnO_2:Sb (Sb doped in SnO_2) [8], Si:B [16], Si:P [16], Tungsten [3], and Molybdenum [5, 20]. The maximum operating temperatures of Pt and Ti are 600°C [16] and 700°C [15]. SnO_2:Sb and poly-silicon materials have temperature limits up to 1000°C, but require high voltage input due to their high resistivity [8]. Tungsten also has a high temperature operation range of 1200°C, however tungsten is only stable in an oxygen-enriched environment up to 400°C [16]. Molybdenum like Tungsten suffers significant oxidation at temperatures of 300°C, which becomes volatile at 700°C, but has capabilities of reaching temperatures of 850°C in a shielded environment [5]. Some material properties in the resistive layer also change with geometry, but the impacts of geometry on resistivity have been shown to be minimal within thin films [4, 11]. Sondheimer theory states that the change in the thickness of the material results in minimal difference in material properties unless the material thickness is less than 8% of its mean-free-path for thin-film metals. This has also been demonstrated experimentally in [21]. Common materials used for oxidation layers are SiO_2, TiO_2, and Al_2O_3/Pt/Ta [16]. These ceramic, silicon, and metal oxide materials have been known to cause high stresses in microheaters [22]. These layers provide many uses in microheaters. They are typically used as insulators to create power efficient microheaters [23]. They're also used for electrical insulation and as a protecting layer [24].

Another material, not shown in the typical configuration, is adhesive materials. Use of adhesives to bond resistors to substrates or oxidative layers is a common practice. Typical materials include Ti, Ta, and Zr [18]. However, at temperatures over 700°C Ti normally will suffer from adhesion issues failing due to the high shear stresses causing the materials to peel off from the resistor or the substrate [25]. The effects of stress have been minimized by using intermediate layers such as Silicon Nitride so that the thermal stress between layers isn't as substantial [26].

2) Modeling

Modeling of microheaters has been used extensively for microheater design. Modeling includes the electrical, thermal, and mechanical characterization of microheaters. An important aspect to the electrical and thermal characterization is the change in materials properties as temperatures are varied. Experiments have been performed to determine the values of materials properties at different temperatures [10]. Resistivity is a material property of particular importance due to its critical role in Joule heating. Materials have a tendency to increase resistivity as temperature increases [27].

Prior research has been performed by experimentation evaluating the effects of heat transfer on microheaters. Microheaters are affected by three types of heat transfer which are conduction, convection, and radiation [6]. It was shown that the effects of conduction and convection can have a significant impact on the heat transfer while radiation is negligible for Ti and Pt materials at temperatures of less than ~700°C [6, 10, 19].

Modeling has also been an essential part of design for microheaters. Modeling has been used to select materials by evaluating the maximum temperature and power savings of microheaters with different insulating layers [9]. In two other studies, modeling was used to study the effects of microheater geometry to improve the evenness of heat distribution. Unique geometries were assessed in [11]. The second study used a spiral pattern, and the effects of the geometric parameters were investigated, such as the filament width and spacing between the filament [12].

3) Design

Many noteworthy design aspects, such as material properties [10], electro-thermal response [9], heat distribution [11], and geometry [12] were found from literature in previous research. K.L. Zhang et al. evaluates the material properties of a Ti/Au microheater. In this study, the design impacts of the materials thermal conductivity, resistivity, and emissivity all have significant impacts on the design. With increase in temperature, the emissivity and resistivity of materials increases while the thermal conductivity decreases [10]. This study also made a comparison of Ti/Au resistors to Pt resistors showing the impacts of thermal expansion and high thermal stress was the typical mode of failure in Ti microheater design. Even heat distribution has been shown to provide power savings by being more efficient and also creates better responses times in microheaters [11]. Thermal response time reached 2ms for high temperature designs of 600°C for Tungsten microheaters with low power consumption of 12mW [3]. A time response of 1ms was achieved in a Pt/Ti heater reaching a temperature of 400°C using only 9mW of power [28].

C. Particle Swarm Optimization

Particle swarm was initially a method of predicting social behavior in animals [29]. This method has been adopted for an extensive amount of applications [30], such as array failure correction for antennas, predictive and tuning controls, design optimization, etc. Particle swarm optimization is an advantageous method. It enables optimization of parameters within a discontinuous problem and with much less computational cost than other optimization method. This is enabled by the method of stochastically searching for the optimal solution [31]. The method evaluates the fitness of a current set of solutions and identifies new design parameters based on a fitness evaluation for minimizing an objective function. Each solution generated moves the parameters closer to the optimal solution at which the numerical problem reaches

convergence [32]. One recent publication utilized particle swarm optimization for design of microheaters to create power savings in microheaters [33]. This application uses basic equations of heat transfer to find the optimal design parameters. The parameters used were the oxide layer thickness, temperature, and active area. Active area is the area of the heat source. No attention was given to optimize for stress nor was the actual geometry of the microheater changed. They also did not consider any constraints, or utilize a finite element model.

III. Modeling Setup and Validation

Modeling of a microheater involves multiple coupling physics. The physical phenomenon experienced in a microheater is that of Joule heating. Joule heating consists of electric currents and heat transfer. In this simulation the structural mechanics involved were also considered which were coupled with heat transfer by thermal expansion.

A. Numerical Modeling

In this section, a model for microheater operation is developed. This section walks through the governing equations used to predict the electrical, thermal, and mechanical response of a microheater.

1) Current conservation

Joule heating is created by running current through a resistive material. The constitutive relationship for the resistive material is described by Ohm's Law:

$$\boldsymbol{J} = \sigma \boldsymbol{E}$$

Equation 1

$\boldsymbol{J}$ is the current density, **E** is the electric field strength, and σ is the electrical conductivity:

$$\sigma = \frac{1}{p_r} = \frac{1}{p_{r,0[1+\alpha(T-T_0)]}}$$

Equation 2

where p_r represents the electrical resistivity, α is the temperature coefficient of resistivity with the assumption that the resistivity changes linearly with temperature, and $(T - T_0)$ is the change in temperature of the resistive material.

Based on charge conservation and equation of continuity, the electric potential throughout the microheater can be described by:

$$-\nabla_t \cdot d(\sigma \nabla_t V) = 0$$

Equation 3

where d is the layer thickness, V is the electrical potential applied, and ∇_t denotes the gradient operator in the tangential direction of the electric field. Resistive heating is induced from the resistivity in the circuit opposing electron flow. This opposition creates heat that can be shown by:

$$Q = \sigma |\nabla_t V|^2$$

Equation 4

where Q is the heat being generated. The equations are coupled together based on the governing equations dependency on other physical phenomenon.

2) Heat Transfer

Heat transfer follows the law of thermodynamics. In microheaters, heat produced by Joule heating is primarily transferred away by conduction and convection for temperature below

700 ˚C. Since only these forms of heat transfer are present, the first law of thermodynamics ultimately reduces to the governing equation for heat transfer:

$$\rho C_p \left(\frac{\partial T}{\partial t}\right) - \nabla \cdot (k\nabla T) - h\nabla T = Q$$

Equation 5

The variables quantifying this equation are the density ρ, specific heat C_p, thermal conductivity k, convection coefficient *h,* change in temperature ∇T, and heat source Q. $\frac{\partial T}{\partial t}$ represents the change of temperature with respect to time and ∇ is the gradient operator.

3) Structural Mechanics

Stress is induced in microheaters as a result of thermal expansion when materials experience a rise in temperature. The governing equation for the structural mechanics is:

$$\frac{\rho(\partial^2 \boldsymbol{u})}{\partial t^2} = \nabla \cdot s + \boldsymbol{F}\mathrm{v}$$

Equation 6

where s is the stress tensor, $\boldsymbol{u}$ is material displacement, and **F**v is the volume force vector.

Computational cost of modeling microheaters can be extensive due to the large ratio of the thickness of the resistive material layer (typically ~200 nm) to that of the substrate (~ 25 μm), which could cause significant meshing issues. One way to simplify is by using the shell theory. Structural mechanics shell theory is different from three dimensional structural mechanics in that the models are formulated by using the Lagrange continuum mechanics with mixed interpolation of tensor components. This reduces computations to consider only plane stress since other stresses will have minimal impact. The mechanical stress is formulated as:

$$\frac{\rho(\partial^2 \boldsymbol{u}_2)}{\partial t^2} = \nabla \cdot \sigma + Fv + \frac{6(M_v \times n)z}{d^2} \&$$

Equation 7

$$\sigma_z = 0$$

Equation 8

where σ is the in plane stress, $(M_v \times n)$ is the volume moment vector, z is the vertical direction, and d is the overall thickness of the shell. The stresses induced in the design are all resultants of thermal expansion which is shown from the thermal strain as:

$$\varepsilon_{th} = \alpha_{th}(T - T_0) \&$$

Equation 9

$$x_{th} = \frac{\alpha_{th}(T - T_0)}{d}$$

Equation 10

where x_{th} corresponds to the strain subject to the bending stress in the shell from thermal expansion, $\varepsilon_{th}$is the strain in the entire domain from thermal expansion, and α_{th} is the thermal coefficient of expansion. The thermal expansion can be coupled to Equation 6 and Equation 7 using the stress-strain relationship of materials.

B. Validation of Numerical Model

The numerical model was implemented using COMSOL 5.1. A multiphysics model was developed for a Pt miroheater on an alumina composite substrate by coupling three physics

involved (i.e., electrical, mechanical, and thermal). This study evaluated the temperature change in the microheater and substrate. To form a solution the numerical model was evaluated transiently.

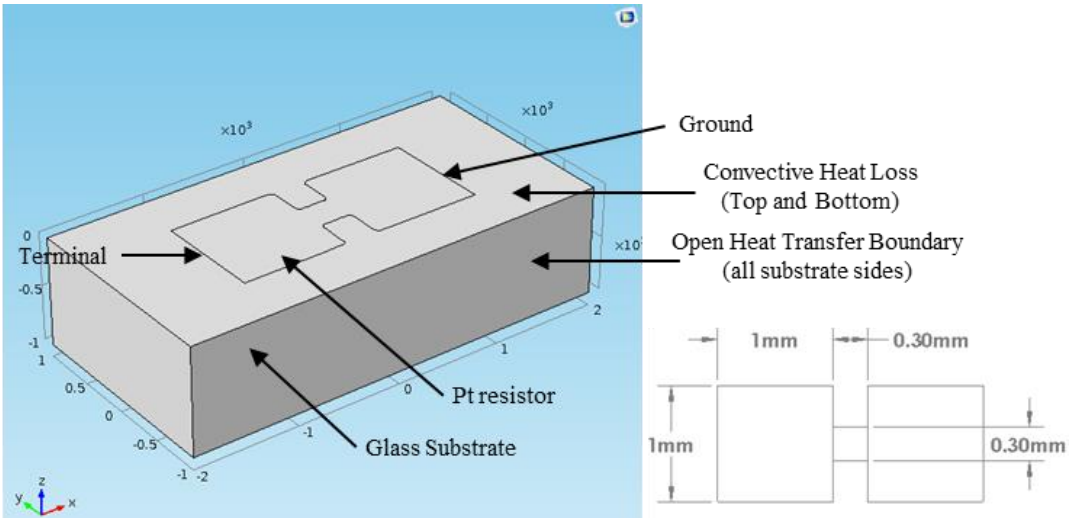

Figure 2-Heater geometry and Boundary Conditions

Table 1-Material Properties of for the 1st Numerical Model Validation

Summary	Pt	Al_2O_3
Specific Heat (J/kg*K)	133	800
Thermal conductivity (W/m*K)	71.6	25
Coefficient of Thermal Expansion (1/K)	8.80E-06	6.50E-06
Density (kg/m^3)	21450	3780
Temperature Coefficient of Resistance (1/K)	3.93E-03	-
Resistivity (Ω*m)	8.33E-07	-
Young's Modulus (Pa)	1.68E+11	4.00E+11
Poisson's Ratio	0.38	0.22
Function	resistor	substrate
Thickness (μm)	0.6	1000

Figure 2 and Table 1 show the initial setup of the numerical model, where the shell boundaries of the Pt resistor were centrally located on the substrate. The open boundary condition was placed on the boundary where the domain would be continuous. This assumes $q|_{x=boundary} = 0$ so the temperatures of the un-modeled part have continuous temperature change at the boundary. The convective heat loss coefficient applied to all other sides was 5W/m*K, which has been commonly used in literature [9, 10]. Table *1* shows the material properties.

The model was validated by comparing the simulation results with the experimental data obtained from literature [9], which are shown in Figure 3. The change of temperature at the center of the microheater after 200 *ms* with respect to input voltage was compared. As we can see, the results have an excellent agreement between our numerical simulations and the experimental data from literature.

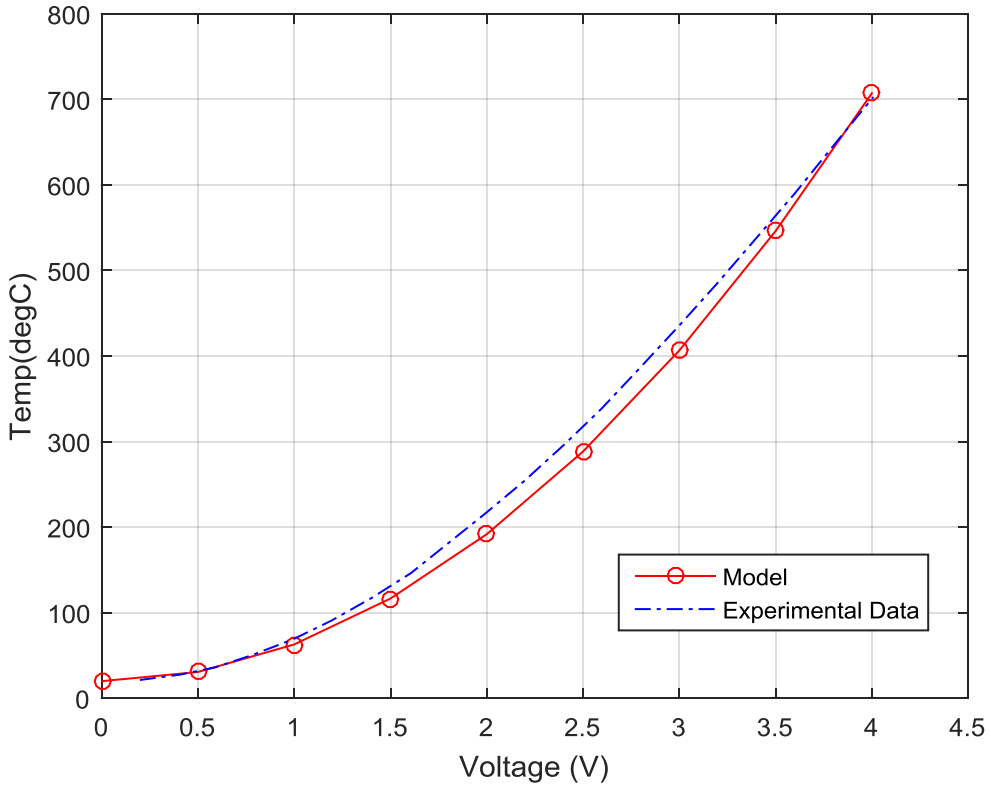

Figure 3-Change of Microheater Vemperature with Voltage Input of Numerical Simulation Compared with Experimental Data

A second validation was also performed on the transient response of the microheater over time because of the importance of transient behavior of a microheater. Simulations of a Ti/Au resistor on a 7740-Pyrex glass substrate were performed to compare with experimental results and other modeling results from literature [10].To simplify this model the conductor layer composed of Au/Ti was modeled as two resistors in parallel. This was assumed due to the parallel orientation in which the materials were stacked and current was supplied through the conductive layer. The convection coefficient used in this model was 100W/m*K [10]. The simulation configuration and material properties are shown in Figure 4 and Table 2 respectively.

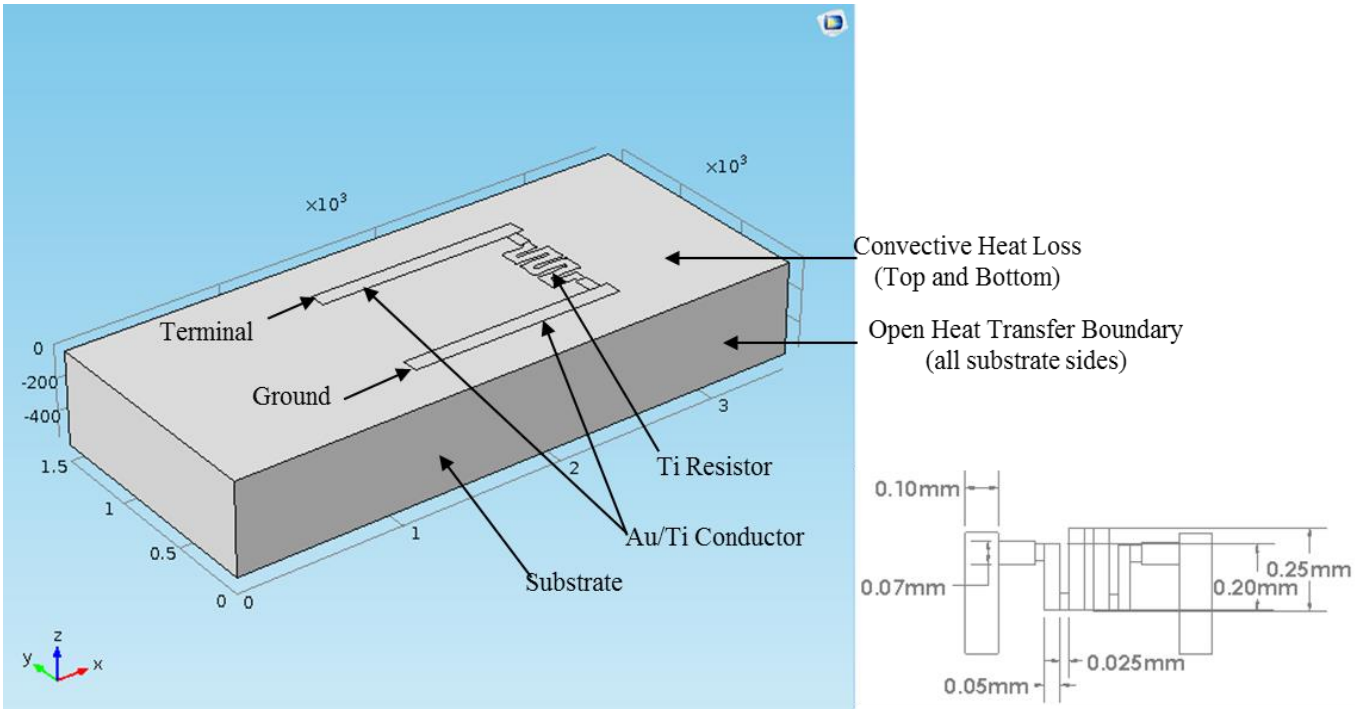

Figure 4-Model Setup of Ti/Au microheater on an Ultra -thin Glass Substrate

Table 2- Material Properties of the 2nd Simulation for Validation

Summary	Pyrex-7740	Au	Ti
Electrical Resistivity (Ω*m)	1.26E+06	3.99E-08	1.54E-06
Thermal Conductivity (W/m*K)	1.18	1.76E+02	5.8
Specific Heat (J/kg*K)	753.12	0.3	131
Density (kg/m^3)	2230	19320	4507
Temperature Coefficient of Resistance (1/K)	-	3.40E-03	1.30E-03
Young's Modulus (Pa)	1.16E+11	6.40E+10	7.00E+10
Poisson's ratio (1)	0.321	0.2	0.44
Thermal Expansion Coefficient (1/K)	8.60E-06	3.25E-06	1.42E-05
Function	Substrate	Conductor	Resistor
Thickness (µm)	550	0.077	0.206

Having setup the numerical model, solutions were then created to form a validation. A 3V potential difference was placed on the resistor, and then the temperature at the hottest point over the entire microheater configuration was extracted at each time step. The transient temperature change over time was compared to previous experimental and modeling results shown in Figure *5* [10]. From comparison, we can see a good agreement. The model being validated agrees more closely with the experimental data as it approaches a steady state than the results from the previous model [10].

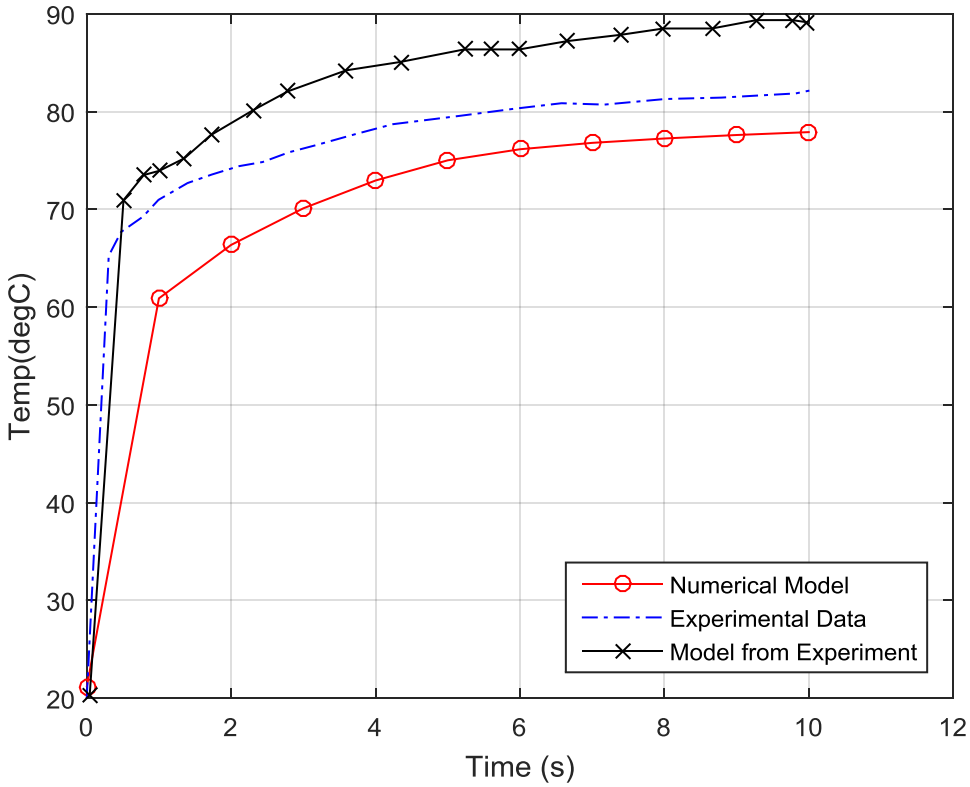

Figure 5-Comparison of Numerical Model to Previous Research for 2nd Validation

IV. OPTIMIZATION

In this section, a particle swarm optimization method was developed to optimize the microheater design in order to minimize its thermal stress and even heat distribution during operation. An initial design was first established and design parameters were identified. The validated numerical model was then employed to evaluate different designs with respect to the optimization objective (i.e., minimal stress, even heat distribution). A particle swarm optimization method was then developed to search for the optimal design in the design space.

A. Initial Design and Design Variables

Based on our literature review, an initial design of the microheater was chosen as follows. An Ultra-thin Glass (type AF 32*eco from Schott Inc.) was used as the substrate to support the resistive filament and conductive pads. This material was chosen due to its low thermal making it power efficient [10]. It also has a transition temperature of 717ºC making it capable of reaching the desired operating temperature range before reaching the transition temperature. Titanium was chosen as the resistive material because of its capability of reaching temperatures in excess of 600°C. Its failure from thermal stress is often the limiting factor, but not until temperatures are in excess of 700°C. Gold was chosen due to its high electrical conductivity. Gold also has low coefficient of thermal expansion, as compared to other popular conductors like silver, which induces less stress in the design. The material properties are listed in .

Table *3-Properties* and Characteristics of the Materials Used for the Initial Design [10, 34]

Summary	Titanium (Ti)	Ultra-thin Glass	Gold(Au)
Electrical Resistivity (Ω*m) @ 20°C	1.54E-06	-	2.77E-08
Temperature Coefficient of Resistance (1/°C)	3.50E-03	-	0.0034
Thermal Expansion Coefficient (1/K)	8.60E-06	3.2E-06	1.42E-05
Thermal Conductivity (W/m*K)	21.9	1.16	3.17E+02
Specific Heat (J/kg*K)	522	820	129
Density (kg/m^3)	4507	2430	19300
Young's Modulus (Pa)	1.16E+11	7.29E+10	7.00E+10
Poisson's ratio (1)	0.321	0.208	0.44
Thickness (µm)	0.2	50	0.2
Purpose	Resistor	Substrate	Conductor

.

Table 3-Properties and Characteristics of the Materials Used for the Initial Design [10, 34]

Summary	Titanium (Ti)	Ultra-thin Glass	Gold(Au)
Electrical Resistivity (Ω*m) @ 20°C	1.54E-06	-	2.77E-08
Temperature Coefficient of Resistance (1/°C)	3.50E-03	-	0.0034
Thermal Expansion Coefficient (1/K)	8.60E-06	3.2E-06	1.42E-05
Thermal Conductivity (W/m*K)	21.9	1.16	3.17E+02
Specific Heat (J/kg*K)	522	820	129
Density (kg/m^3)	4507	2430	19300
Young's Modulus (Pa)	1.16E+11	7.29E+10	7.00E+10
Poisson's ratio (1)	0.321	0.208	0.44
Thickness (µm)	0.2	50	0.2
Purpose	Resistor	Substrate	Conductor

The initial geometric design established was obtained from [11]. It was demonstrated to be capable of creating a minimal temperature deviation across the design space. Figure 9 shows the initial design. The outer radius determines the size of the microheater and was chosen to be 50um for this study. The initial values of the rest of the design parameters are listed in Table 4.

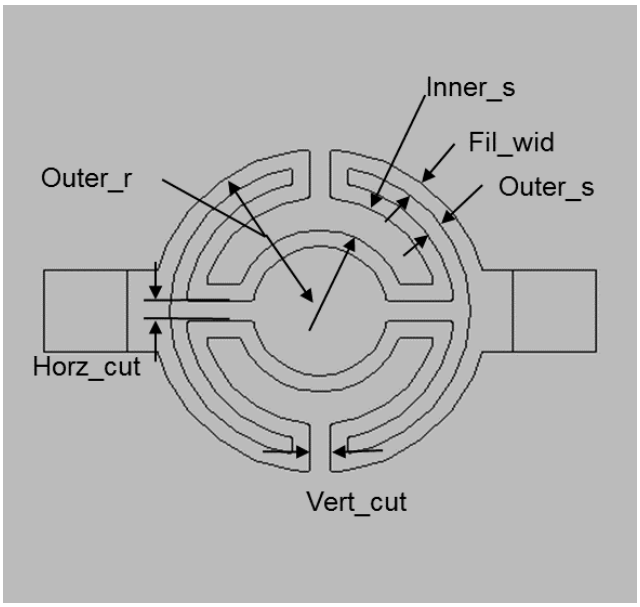

Figure 6-Design Parameters Describing Topology of the Resistor

Table 4-Initial Values of the Design Parameters

Parameter	Value	Unit	Description
Fil_wid	12.5	Um	Filament Width
Outer_s	27.5	Um	Outer Spacing
Vert_cut	25	Um	Vertical Cut
Horz_cut	12.5	Um	Horizontal Cut
Inner_s	10	Um	Inner Spacing
Fil_thick	200	Nm	Filament Thickness

B. Particle Swarm Optimization

With the six design parameters chosen, we needed to determine the optimal combination of the design parameters in the six-dimensional design space. Because it was impossible to test every design in the design space, an efficient method was needed to search for the optimal design. Particle swarm optimization has established itself as a popular method of design optimization. This method stochastically searches for an optimal solution within a specified design space by changing the design parameters. We developed a unique method for constraining particle swarm algorithms as well as using complex models within the algorithms. This is a new concept to microheater design. In this section, we will use constrained particle swarm optimization to search for optimal topology solutions using the variables initially established in the geometry.

Particle swarm optimization randomly searches for solutions to problems within a design space. In this algorithm, each particle is a design with a set of design parameters (i.e., the six design parameters in Table 4. The lower bound and upper bound of the design parameters determine the boundaries of the design space. Each particle has its own unique position and velocity in the design space. The velocity is determined by the particle's personal best and the global best of all particles and used to updates the particle's current position based on:

$$v = v_i + c1 * rand( ) * (pbest - present) + c2 * rand( ) * (gbest - present)$$
Equation 11

Where c1=c=2 and are arbitrary constants, pbest is the personal best of the particle, rand is a random number from [0,1], gbest is the overall best is the algorithm, present is the present solution, and v_i is the current velocity.

The validated finite element model was used to evaluate the fitness of each particle with respect to the design objectives. The algorithm randomly generates initial particles and moves the particles in the design space based on their velocities. This stochastic search enables convergence of optimization algorithms for complex problems such as a microheater design. Certain designs are undesirable for the microheater, which were accounted for by placing constraints on the particles. One constraint was that we want the total resistance of the microheater to be above 100 Ω so that the heat concentrates on the microheater instead of on the external circuit. Another constraint was used to ensure geometric continuity in the design. With the stochastic search, the algorithm outputs the optimal design, $x_{optimal}$, and minimized objective function, f_{min}.

The pseudo ,code of the particle swarm algorithm is presented below.

1 Initialize function [$x_{optimal}, f_{min}$] defining the boundary of the design parameters
2 Randomly generate initial particles // each particle is a design
3 Check Resistance of the design //initial constraint
4 If Resistance>100Ω; continue
5 If geometry is continuous; continue
6 Else; go to step 2
7 Evaluate the generated particles using COMSOL
8 Find the best particle from initially generated particles
9 For i= 1: # of iterations
10 Move the particles based on their velocities calculated from *Equation 11*
$x_{n+1} = x_n + v$ where x_n is the position of the particle
11 Check resistance (updated particles)
12 If R>100; continue
13 If geometry is continuous; continue
14 Else; go to step 9
15 Evaluate updated particles using COMSOL
16 If; objective function value< previous objective function value, update particle position
17 Else; keep previous particles
18 Keep best particle
19 Update the velocities for each particle
20 Evaluate iteration number
21 If i>max iteration; go to step 23
22 Else keep best value; go to step 7
23 Solution=[$x_{optimal}, f_{min}$]

24 End

C. Results and Discussion

Boundaries of each design parameter are defined in Table 5. The first objective function was to minimize the maximum stress over the entire microheater. Only thermal stresses in the substrate are accounted for in this design. Stress is sometimes induced in the devices from fabrication methods and exist in other parts of the microheater (i.e. filament, adhesive interface), but are not taken into account here. The second objective function was to create even heat distribution by minimizing the standard deviation of temperature within 121 evenly distributed sample points over the entire microheater. The amount of sample points used to evaluate the model was determined to be sufficient in this study. Even heat distribution was accomplished within the sample space by optimizing variables input to the optimization algorithm. For the simulations, power was supplied at 1W for 1 *ms*. The simulation creates a temperature of ~600ºC within the design for both objectives. Results from optimization are in Table 6 and Table 7.

Table 5-Upper and Lower Bounds of Design Parameters used for Optimization

x values in µm	Fil_wid	Outer_s	Vert_cut	Horz_cut	Inner_s	Fil_thick
lb	4	7	7	7	10	0.15
ub	4.25	10	11	11	17	0.2

Table 6-Initial and Optimal Design Parameters

x values in µm	Fil_wid	Outer_s	Vert_cut	Horz_cut	Inner_s	Fil_thick
Initial	4	7	11	10	13	0.2
Optimal Stress	4.2	9.9	11	10	12.9	0.2
Optimal Heat Distribution	4	8	10	10.7	16	0.2

Table 7-Values Obtained for the Initial and Optimal Design

Values	Optimal Stress (MPa)	Optimal Heat Distribution (degC)
Initial	92.1	92.2
Optimal	88.7	90

The stress resulting from the difference in thermal expansion in the materials was reduced from 92.1 MPa to 88.7 MPa. This is within the yield strength of the Ultra-thin glass making this a feasible design. For even heat distribution, the initial design had standard deviation of 92.2ºC and was reduced to 90ºC. Results from the single objective optimization problems were compared as shown below Figure 7. Differences in the geometry can be seen from Table 6, but the values obtained for the solutions show little difference compared to the initial design. This may suggest that a larger design space should be used. This will enable a greater variation in results by adding or redefining the design parameters.

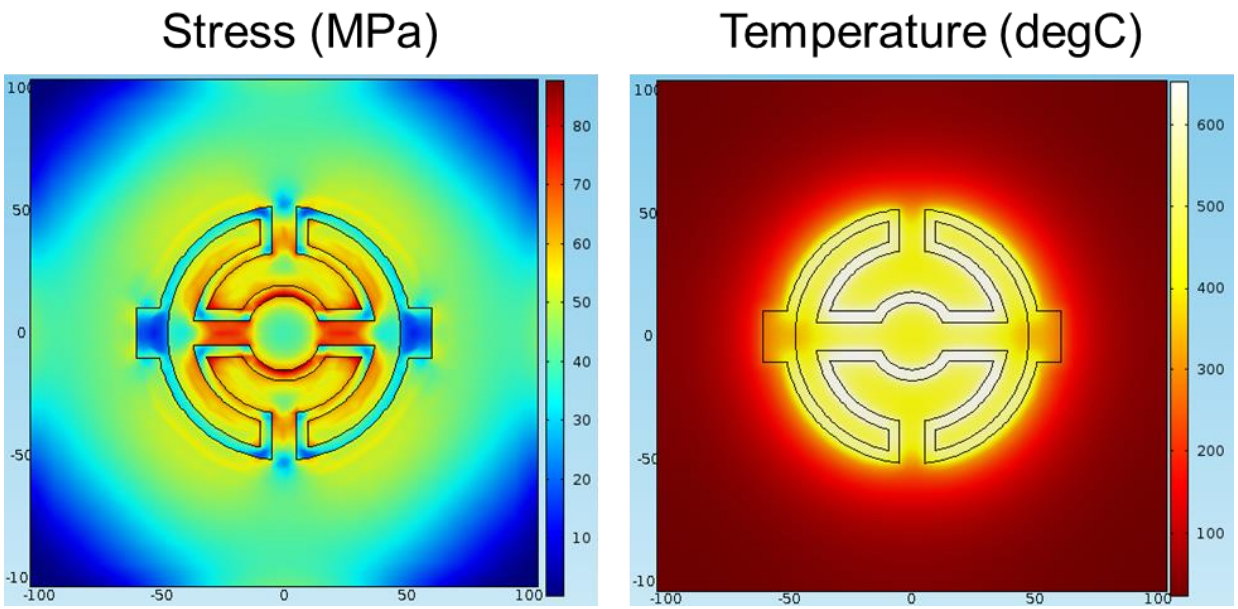

Figure 7-Comparing Optimal Solution of Minimizing Stress with Even Heat Distribution

A particular point of interest in this study was the convergence and solve time of the algorithm. The algorithm used 10 particles and 10 iterations which was determined in the study to be enough by comparison. Negligible differences in results were found for 25 iterations when compared to 10 iterations. Even heat distribution optimization took 2 hours to solve and minimizing stress took 8 hours and 42 minutes to solve. Each iteration the overall best solution was recorded and plotted against the iteration number to show the convergence. A convergent plot shows the optimization method used arrives at a minimum of the objective function. From this we learn that this algorithm not only converges, but that it converges quickly, within 10 iterations.

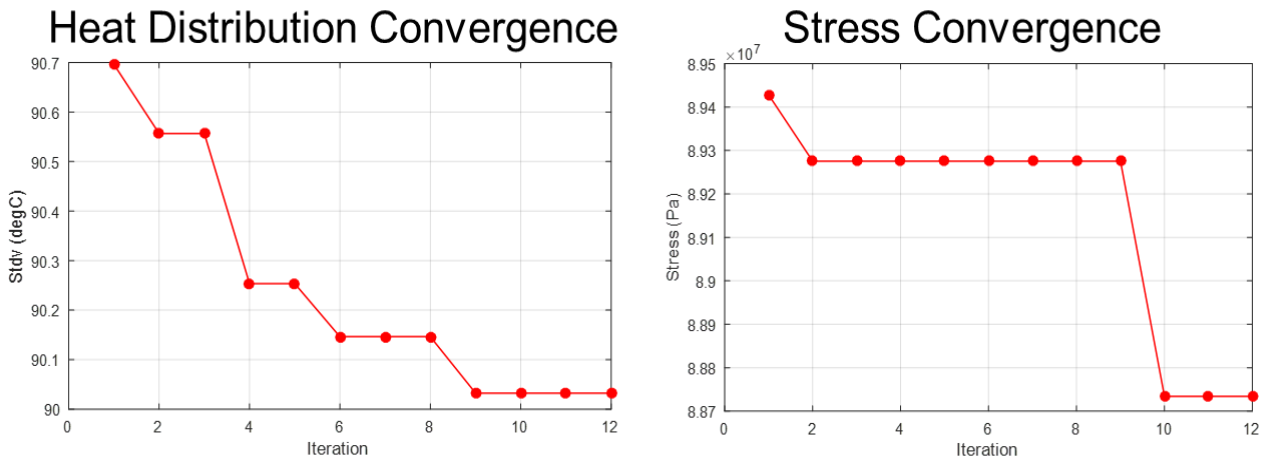

Figure 8-Convergence of Optimization Problems

V. Conclusion

This paper was set out to develop an optimization algorithm for designing a high temperature microheater for thermal inkjet. First, a literature review was provided on previous research on microheater design, fabrication, and operation. A multiphysics model was developed to simulate microheater operation and evaluate microheater design, which was then validated with experimental data from literature. To optimize the microheater design, an initial geometry with set of design parameters were identified. A particle swarm optimization algorithm was then developed to search for optimal design using the experimentally validated multiphysics model to evaluate different designs. Optimal designs were found for two different objective functions, minimal stress and even heat distribution. The developed algorithm was demonstrated to be an effective and efficient tool for optimizing microheater designs. The results obtained for both objectives were shown to be very similar, which could both serve as a good microheater design for high temperature operations for thermal inkjet.

VI. Acknowledgements

We would like to thank my colleagues in AM^3 Lab for providing support and a productive learning environment for conducting these studies and writing this paper. We gratefully acknowledge the financial support from the University of Arkansas, through the startup fund provided by the Vice Provost Office for Research and Economic Development. Any opinions, findings, and conclusions or recommendations expressed in this publication are those of the authors and do not necessarily reflect the views of the University of Arkansas.

References

[1] L. Setti, C. Piana, S. Bonazzi, B. Ballarin, D. Frascaro, A. Fraleoni-Morgera and S. Giuliani, "Thermal inkjet technology for the microdeposition of biological molecules as a viable route for the realization of biosensors," *Anal. Lett.,* vol. 37, pp. 1559-1570, 2004.

[2] W. Zhou, "Interface dynamics in inkjet deposition," 2014.

[3] S. Z. Ali, F. Udrea, W. I. Milne and J. W. Gardner, "Tungsten-based SOI microhotplates for smart gas sensors," *Microelectromechanical Systems, Journal Of,* vol. 17, pp. 1408-1417, 2008.

[4] F. Lacy, "Investigating thin films for use as temperature sensors," in *Proceedings of the World Congress on Engineering & Computer Science: October 24-26,* 2007, pp. 441-444.

[5] L. Mele, F. Santagata, E. Iervolino, M. Mihailovic, T. Rossi, A. Tran, H. Schellevis, J. Creemer and P. Sarro, "A molybdenum MEMS microhotplate for high-temperature operation," *Sensors and Actuators A: Physical,* vol. 188, pp. 173-180, 2012.

[6] A. Pike and J. W. Gardner, "Thermal modelling and characterisation of micropower chemoresistive silicon sensors," *Sensors Actuators B: Chem.,* vol. 45, pp. 19-26, 1997.

[7] S. Semancik, R. Cavicchi, M. Wheeler, J. Tiffany, G. Poirier, R. Walton, J. Suehle, B. Panchapakesan and D. DeVoe, "Microhotplate platforms for chemical sensor research," *Sensors Actuators B: Chem.,* vol. 77, pp. 579-591, 2001.

[8] J. Spannhake, A. Helwig, G. Müller, G. Faglia, G. Sberveglieri, T. Doll, T. Wassner and M. Eickhoff, "SnO 2: Sb–A new material for high-temperature MEMS heater applications: Performance and limitations," *Sensors Actuators B: Chem.,* vol. 124, pp. 421-428, 2007.

[9] S. Toskov, R. Glatz, G. Miskovic and G. Radosavljevic, "Modeling and fabrication of pt micro-heaters built on alumina substrate," in *Electronics Technology (ISSE), 2013 36th International Spring Seminar On,* 2013, pp. 47-52.

[10] K. Zhang, S. Chou and S. Ang, "Fabrication, modeling and testing of a thin film Au/Ti microheater," *International Journal of Thermal Sciences,* vol. 46, pp. 580-588, 2007.

[11] S. Lee, D. Dyer and J. Gardner, "Design and optimisation of a high-temperature silicon micro-hotplate for nanoporous palladium pellistors," *Microelectron. J.,* vol. 34, pp. 115-126, 2003.

[12] G. Velmathi, N. Ramshanker and S. Mohan, "Design, electro-thermal simulation and geometrical optimization of double spiral shaped microheater on a suspended membrane for gas sensing," in *IECON 2010-36th Annual Conference on IEEE Industrial Electronics Society,* 2010, pp. 1258-1262.

[13] (). *James Prescoot Joule* [James Prescott Joule]. Available: http://www.sciencemuseum.org.uk/onlinestuff/people/james%20prescott%20joule.aspx.

[14] (). *Timeline of Our History* [HP Timeline]. Available: http://www8.hp.com/us/en/hp-information/about-hp/history/hp-timeline/timeline.html.

[15] J. Creemer, D. Briand, H. Zandbergen, W. Van der Vlist, C. de Boer, N. F. de Rooij and P. Sarro, "Microhotplates with TiN heaters," *Sensors and Actuators A: Physical,* vol. 148, pp. 416-421, 2008.

[16] R. M. Tiggelaar, "Silicon-technology based microreactors for high-temperature heterogeneous partial oxidation reactions," 2004.

[17] Y. S. Kim, "Microheater-integrated single gas sensor array chip fabricated on flexible polyimide substrate," *Sensors Actuators B: Chem.,* vol. 114, pp. 410-417, 2006.

[18] T. Maeder, L. Sagalowicz and P. Muralt, "Stabilized platinum electrodes for ferroelectric film deposition using Ti, Ta and Zr adhesion layers," *Japanese Journal of Applied Physics,* vol. 37, pp. 2007-2012, 1998.

[19] D. Bradley and A. Entwistle, "Determination of the emissivity, for total radiation, of small diameter Platinum-10% Rhodium wires in the temperature range 600-1450 C," *British Journal of Applied Physics,* vol. 12, pp. 708, 1961.

[20] G. Gordillo, F. Mesa and C. Calderón, "Electrical and morphological properties of low resistivity Mo thin films prepared by magnetron sputtering," *Brazilian Journal of Physics,* vol. 36, pp. 982-985, 2006.

[21] K. L. Chopra, "Thin film phenomena," 1969.

[22] T. Demirci, D. Guney, A. Bozkurt and Y. Gurbuz, "Electro-thermal simulations and modelling of micromachined gas sensor," in *Microelectromechanical Systems Conference, 2001,* 2001, pp. 99-102.

[23] C. Rossi, P. Temple-Boyer and D. Estève, "Realization and performance of thin SiO 2/SiN x membrane for microheater applications," *Sensors and Actuators A: Physical,* vol. 64, pp. 241-245, 1998.

[24] K. Zhang, C. Rossi, M. Petrantoni and N. Mauran, "A nano initiator realized by integrating Al/CuO-based nanoenergetic materials with a Au/Pt/Cr microheater," *Microelectromechanical Systems, Journal Of,* vol. 17, pp. 832-836, 2008.

[25] R. Srinivasan, I. Hsing, P. E. Berger, K. F. Jensen, S. L. Firebaugh, M. A. Schmidt, M. P. Harold, J. J. Lerou and J. F. Ryley, "Micromachined reactors for catalytic partial oxidation reactions," *AIChE J.,* vol. 43, pp. 3059-3069, 1997.

[26] X. Zhang and C. P. Grigoropoulos, "Thermal conductivity and diffusivity of free- standing silicon nitride thin films," *Rev. Sci. Instrum.,* vol. 66, pp. 1115-1120, 1995.

[27] R. B. Belser and W. H. Hicklin, "Temperature coefficients of resistance of metallic films in the temperature range 25 to 600 C," *J. Appl. Phys.,* vol. 30, pp. 313-322, 1959.

[28] Y. Mo, Y. Okawa, K. Inoue and K. Natukawa, "Low-voltage and low-power optimization of micro-heater and its on-chip drive circuitry for gas sensor array," *Sensors and Actuators A: Physical,* vol. 100, pp. 94-101, 2002.

[29] R. C. Eberhart and J. Kennedy, "A new optimizer using particle swarm theory," in *Proceedings of the Sixth International Symposium on Micro Machine and Human Science,* 1995, pp. 39-43.

[30] R. Poli, "An analysis of publications on particle swarm optimization applications," 2007.

[31] G. Venter and J. Sobieszczanski-Sobieski, "Particle swarm optimization," *AIAA J.,* vol. 41, pp. 1583-1589, 2003.

[32] I. C. Trelea, "The particle swarm optimization algorithm: convergence analysis and parameter selection," *Information Processing Letters,* vol. 85, pp. 317-325, 2003.

[33] B. Kantha and S. K. Sarkar, "Comparative Study of Particle Swarm Optimization and Genetic Algorithm for the Optimization of System Parameters of MEMS Based Micro-Heater," *Journal of Computational and Theoretical Nanoscience,* vol. 12, pp. 1641-1646, 2015.

[34] R. B. Belser and W. H. Hicklin, "Temperature coefficients of resistance of metallic films in the temperature range 25 to 600 C," *J. Appl. Phys.,* vol. 30, pp. 313-322, 1959.